

# Formulation and Evaluation of Orodispersible Tablet of Desloratadine By Applying Taste Masking Technology

Phanse V. R<sup>1\*</sup>, Silawat N<sup>1</sup>.

<sup>\*1</sup>Department of Pharmacy, Oriental University, Indore, Madhya Pradesh- 453555, India

Received: 10<sup>th</sup> Aug, 2025; Revised: 5<sup>th</sup> Sep 2025; Accepted: 13<sup>th</sup> Nov, 2025; Available Online: 30<sup>th</sup> Nov, 2025

## ABSTRACT

**Objectives:** To develop and optimize taste-masked orodispersible tablets of desloratadine using ion-exchange resin complexation technology for enhanced patient compliance and therapeutic efficacy in allergic rhinitis management.

**Materials and methods:** Drug-resin complexes were prepared using Indion 204 at various ratios and characterized by FTIR and DSC. Orodispersible tablets were formulated using 3<sup>2</sup> factorial design with Kyron T-314 (0.75-2.25 mg) and sodium starch glycolate (6-12 mg) as independent variables. Response surface methodology optimized hardness and disintegration time. Pharmacokinetic studies compared optimized formulation with marketed tablets in Wistar rats.

**Results:** Indion 204 achieved optimal drug loading (98.4%) at 1:4 ratio with confirmed molecular interactions. Formulation F9 was selected as optimal based on minimal hardness (1.76 Kg/cm<sup>2</sup>) and rapid disintegration (24.1 seconds) predicted by quadratic models (R<sup>2</sup> >0.86). F9 demonstrated superior dissolution (95.8% in 15 minutes), enhanced bioavailability (268.13% relative), reduced Tmax (2.17 hours), and excellent stability over six months with acceptable f<sub>2</sub> similarity factors (≥50).

**Conclusion:** The optimized formulation successfully addresses critical compliance issues through effective taste masking and rapid drug delivery, offering significant clinical advantages for pediatric and geriatric populations. This patient-friendly approach demonstrates strong potential for clinical translation and commercial development, warranting human bioequivalence studies and scale-up optimization.

**Keywords:** Desloratadine, orodispersible tablets, taste masking, ion-exchange resin, factorial design, response surface methodology, bioavailability enhancement.

**How to cite this article:** Phanse VR, Silawat N, Formulation and Evaluation of Orodispersible Tablet of Desloratadine by Applying Taste Masking Technology. *Int J Drug Deliv Technol.* 2025;15(4): 1650-1665, DOI: 10.25258/ijddt.15.4.17

**Source of support:** Nil.

**Conflict of interest:** None

## INTRODUCTION

Allergic rhinitis remains a significant global health burden, affecting approximately 400 million individuals worldwide with prevalence rates ranging from 10-40% in adults and exceeding 40% in pediatric populations, demonstrating an annual increase of 3-5% in emerging economies particularly in urban areas where rates approach 45%<sup>1</sup>. Recent epidemiological data from 2023-2024 indicates the economic burden exceeds USD 25 billion annually in direct healthcare costs alone, with individual patient expenditures ranging from USD 350-1,200 yearly depending on disease severity and geographical location<sup>2</sup>. Current oral antihistamine therapies demonstrate suboptimal compliance rates of 43-57%, primarily attributed to swallowing difficulties affecting 35% of adults and 50% of pediatric patients, coupled with delayed therapeutic onset requiring 45-60 minutes for symptom relief<sup>3</sup>. The pediatric and geriatric populations, representing 38% of allergic rhinitis patients globally, face particular challenges with conventional tablet formulations, creating substantial treatment gaps that contribute to disease progression with 30-40% of untreated cases advancing to asthma within 8-10 years<sup>4</sup>. Emergency department visits for severe allergic reactions have increased by 18% since 2021, with recent

market analyses projecting continued growth in allergic rhinitis prevalence through 2032, emphasizing the urgent need for rapidly acting, patient-friendly antihistamine formulations that ensure consistent therapeutic outcomes across diverse patient populations<sup>5</sup>.

Desloratadine, chemically designated as 8-chloro-6,11-dihydro-11-(4-piperidinylidene)-5H-benzo[5,6]cyclohepta[1,2-b]pyridine, represents a second-generation tricyclic histamine H<sub>1</sub>-receptor antagonist demonstrating superior efficacy with minimal sedative effects compared to first-generation antihistamines<sup>6</sup>. The compound exhibits exceptional receptor selectivity with Ki values of 0.9-2.3 nM for H<sub>1</sub>-receptors while showing negligible anticholinergic or antiserotonin activities, substantially reducing adverse effects commonly encountered with older antihistamines<sup>7</sup>. Recent clinical evaluations confirm that once-daily 5mg doses achieve 85-90% symptom reduction within 24 hours, maintaining therapeutic plasma concentrations through its active metabolite 3-hydroxydesloratadine, with bioavailability reaching 70-80% ensuring reliable therapeutic outcomes<sup>8</sup>. Pharmacokinetic studies conducted in 2023 demonstrated that pediatric populations aged 2-11 years achieve median AUC values of 38.2-38.8 ng·mL<sup>-1</sup>·h following appropriate

\*Author for Correspondence: vishalrphanse1984@gmail.com

dose adjustments, confirming safety and efficacy comparable to adult exposures<sup>9</sup>. However, desloratadine exhibits intensely bitter taste with a threshold value of 0.05 mg/mL, significantly impacting patient acceptability particularly in pediatric formulations where taste preferences critically influence adherence, necessitating innovative pharmaceutical approaches to mask this unpleasant organoleptic property while maintaining therapeutic efficacy and bioequivalence<sup>10</sup>.

Orodispersible tablet technology combined with ion-exchange resin complexation offers an innovative delivery platform addressing both taste masking and rapid drug release requirements, with the global ODT market projected to reach USD 31.80 billion by 2034 reflecting an 8.15% annual growth rate<sup>11</sup>. Recent formulation studies in 2024 demonstrate that pharmaceutical-grade weak cation exchange resins including Kyron T-114, Indion 204, and Indion 234 achieve 95-98% drug loading efficiency while effectively preventing immediate taste receptor interaction through controlled ionic complexation mechanisms<sup>12</sup>. These resins containing carboxylic functional groups form stable complexes with desloratadine at salivary pH (6.8-7.4), successfully masking bitterness while ensuring complete drug release at gastric pH (1.2-2.0) within 15 minutes, maintaining bioequivalence with conventional formulations<sup>13</sup>. Advanced superdisintegrants including sodium starch glycolate, crospovidone (2-5% w/w), and croscarmellose sodium facilitate rapid tablet dispersion within 30 seconds without water requirement, producing particles below 200 micrometers ensuring optimal mouthfeel and patient acceptability<sup>14</sup>. Recent comparative dissolution studies published in 2024 demonstrate 90-100% drug release within 6-10 minutes for optimized ODT formulations versus 45 minutes for conventional tablets, with direct compression manufacturing technology ensuring scalability at production speeds of 100,000-150,000 tablets hourly while maintaining 24-month stability at ambient conditions, potentially improving medication adherence by 40-50% particularly in pediatric, geriatric, and dysphagic populations<sup>15</sup>.

Building on these technological advances, this study aims to develop and evaluate an optimized orodispersible tablet formulation of desloratadine incorporating comprehensive taste-masking technology through ion-exchange resin complexation. The primary objective focuses on achieving complete taste masking while maintaining rapid disintegration below 30 seconds and bioequivalent drug release profiles compared to conventional formulations. Secondary objectives include establishing optimal drug-resin complexation parameters, evaluating long-term stability under accelerated conditions, and conducting comparative palatability assessments through sensory evaluation.

## MATERIALS AND METHODS

### MATERIALS

Desloratadine (USP grade, 99.5% purity) was purchased in Sciquaint Innovations Pvt. Ltd. (Pune, India). Kyron T-314, beta-cyclodextrin, methanol (HPLC grade) and mannitol were acquired at Sciquaint Chemicals (Pune, India).

Aspartame, pharmaceutical flavoring agents, indion 204, and indion 234 were purchased in Neeta Chemicals (Pune, India). Sodium starch glycolate, magnesium stearate, microcrystalline cellulose, PH-102 and potassium bromide were purchased at Research Lab Fine Chem Industries (Mumbai, India). The chemicals were all USP/analytical grade unless otherwise, and the rest of the reagents were of analytical grade quality.

### METHODS

#### *Determination of Absorption Maxima ( $\lambda_{max}$ )*

The absorption maxima ( $\lambda_{max}$ ) of desloratadine was determined using double beam UV-Visible spectrophotometer (Model UV-2700, Shimadzu Scientific Instruments Pvt. Ltd., Mumbai, India) equipped with 1.0 cm quartz cuvettes. A standard solution (10.0  $\mu\text{g/mL}$ ) was prepared by diluting stock solution with HPLC grade methanol (Merck Specialities Pvt. Ltd., Mumbai, India) and scanned over 200-400 nm range against methanol blank at  $25 \pm 2^\circ\text{C}$ . The scanning parameters included scan speed of 480 nm/min, slit width of 1.0 nm, and sampling interval of 1.0 nm according to ICH Q2(R1) guidelines. The  $\lambda_{max}$  was confirmed by analyzing three concentrations (8.0, 10.0, and 12.0  $\mu\text{g/mL}$ ) and determined in triplicate ( $n=3$ ) for all subsequent quantitative measurements<sup>16</sup>.

#### *Calibration Curve Determination*

The calibration curve was established using a double beam UV-Visible spectrophotometer (Model UV-2700, Shimadzu Scientific Instruments Pvt. Ltd., Mumbai, India) with 1.0 cm quartz cuvettes at ambient temperature ( $25 \pm 2^\circ\text{C}$ ). Primary stock solution (1000.0  $\mu\text{g/mL}$ ) was prepared by dissolving 100.0 mg desloratadine in 100.0 mL HPLC grade methanol (Merck Specialities Pvt. Ltd., Mumbai, India) using ultrasonication for 15 minutes at  $40^\circ\text{C}$ , from which working standards of 2.0-20.0  $\mu\text{g/mL}$  were prepared by serial dilution. The  $\lambda_{max}$  was determined by scanning against methanol blank, followed by absorbance measurements for all standards in triplicate ( $n=3$ ) according to ICH Q2(R1) guidelines. Calibration curve was constructed by plotting absorbance versus concentration<sup>17</sup>.

#### *Drug-Resin Complex Formation Study*

The drug-resin complex formation study was conducted to optimize complexation ratio between desloratadine and ion-exchange resins using batch equilibrium method. Various drug:resin ratios (1:1, 1:2, 1:3, 1:4, 1:5 w/w) were evaluated using Kyron T-114 (Corel Pharma Chem, Ahmedabad, India), Indion 204, and Indion 234 (Ion Exchange India Ltd., Mumbai, India). Accurately weighed desloratadine and resin were dispersed in 50.0 mL distilled water and stirred using magnetic stirrer (Model 2MLH, Remi Equipment Pvt. Ltd., Mumbai, India) at 100 rpm and  $37 \pm 0.5^\circ\text{C}$  for 4 hours with pH maintained at  $6.8 \pm 0.2$  using phosphate buffer. After filtration through Whatman filter paper No. 41, the filtrate was analyzed spectrophotometrically to determine free drug concentration. Drug loading efficiency was calculated as:

$$\text{Drug loading efficiency} = \frac{(\text{Initial drug-Free drug})}{\text{Initial drug}} \times 100$$

with results expressed as mean  $\pm$  standard deviation (n=3) and evaluated using one-way ANOVA<sup>18</sup>.

#### Fourier Transform Infrared Spectroscopy

Fourier Transform Infrared Spectroscopy investigation examined molecular-level interactions and validated complex development between desloratadine and Indion 204 resin utilizing an FTIR-8400S spectrophotometer (Shimadzu Scientific Instruments Pvt. Ltd., Mumbai, India). Analysis encompassed four specimen types: desloratadine in pure state, unmodified Indion 204 resin, physical blend prepared at 1:4 mass proportion, and drug-resin complex synthesized at matching 1:4 ratio. Specimen handling required combining 2-3 mg test material with 200 mg moisture-free potassium bromide followed by pellet formation through hydraulic compression applying 10 tons force sustained for 2 minutes. Spectral acquisition covered 4000-400  $\text{cm}^{-1}$  wavenumber domain employing 4  $\text{cm}^{-1}$  resolution settings, 32-scan signal averaging protocol, and 2 mm/sec scanning velocity at ambient temperature of  $25 \pm 2^\circ\text{C}$  conforming to USP <197> methodology. Characteristic absorption bands underwent comparative assessment targeting position shifts, intensity variations, peak broadening phenomena, or band elimination patterns signifying molecular association events, with experimental design incorporating triplicate determinations (n=3) and data interpretation facilitated through IR Solution software platform<sup>19</sup>.

#### Differential Scanning Calorimetry

Thermal analysis through Differential Scanning Calorimetry employed a DSC-60 Plus instrument (Shimadzu Scientific Instruments Pvt. Ltd., Mumbai, India) operating under nitrogen purge conditions to examine thermal characteristics and verify potential drug-resin interactions. The investigation encompassed four distinct samples: desloratadine in pure form, Indion 204 resin without modification, a physical blend combining drug and resin at 1:4 mass ratio, and the complexed drug-resin system prepared at identical 1:4 proportion. Sample handling required precise measurement of 3-5 mg material portions placed into standard aluminum pans followed by hermetic sealing through aluminum lid application using mechanical sample press. Thermographic recording spanned 30-300°C temperature domain with controlled heating progression at 10°C per minute while maintaining nitrogen gas flow at 50 mL/min rate in accordance with USP <891> specifications. Thermal phenomena including endothermic melting transitions, glass transformation events, and decomposition responses underwent systematic identification with comparative evaluation focusing on peak position alterations, intensity modifications, or signal elimination patterns suggesting drug-resin association. Experimental protocol incorporated triplicate measurements (n=3) utilizing empty aluminum pan for reference baseline, with resulting thermograms subjected to computational processing via TA-60WS software platform enabling peak characterization and thermal parameter quantification<sup>20,21</sup>.

#### Experimental Design

Using the Design-Expert version 13.0, a 3<sup>2</sup> full factorial was designed to optimize the desloratadine orodispersible

tablets, which were to be evaluated through a single experimental run (9) and the independent variables were Kyron T-314 at 0.75 mg (low), 1.5 mg (middle), and 2.25 mg (high), and Sodium Starch Glycolate at 6 mg (low), 9 mg (middle), and 12 mg (high). Hardness ( $R^1$ , kg/cm<sup>2</sup>) and disintegration time ( $R^2$ , seconds) were chosen as the dependent variables, and their values were required to be minimized to attain an optimal pill formation. To determine the relationship between independent and dependent variables in the form of a second-order poly equation, multiple regression analysis was done as follows:

$$Y = \beta_0 + \beta_1A + \beta_2B + \beta_{12}AB + \beta_{11}A^2 + \beta_{22}B^2,$$

where Y denotes the response to be predicted,  $\beta_0$  denotes the intercept,  $\beta_1$  and  $\beta_2$  are linear coefficients,  $\beta_{12}$  is the interaction coefficient, and  $\beta_{11}$  and  $\beta_{22}$  are quadratic coefficients to minimize formulation parameters<sup>22,23</sup>.

**Table 1: Variables and their levels in 3<sup>2</sup> full factorial level.**

Variables	Levels		
	Low	Middle	High
(A) = Kyron T-314 (mg)	0.75	1.5	2.25
(B) = Sodium starch glycolate (mg)	6	9	12
Dependent variables	Goals		
(R <sub>1</sub> ) = Hardness (Kg/cm <sup>2</sup> )	Minimize		
(R <sub>2</sub> ) = Disintegration time (Sec)	Minimize		

**Table 2. Composition of desloratadine orodispersible tablet formulations**

Ingredients (mg)	F 1	F 2	F 3	F 4	F 5	F 6	F 7	F 8	F 9
Desloratadine-Resin complex	25	25	25	25	25	25	25	25	25
Kyron T314	0.75	1.5	2.25	0.75	1.5	2.25	0.75	1.5	2.25
Sodium starch glycolate	6	6	6	9	9	9	12	12	12
Beta-cyclodextrin	80	80	80	80	80	80	80	80	80
Mannitol	10	10	10	10	10	10	10	10	10
Aspartame	1.5	1.5	1.5	1.5	1.5	1.5	1.5	1.5	1.5
Flavor	1.5	1.5	1.5	1.5	1.5	1.5	1.5	1.5	1.5
Magnesium stearate	1	1	1	1	1	1	1	1	1

Microcrystalline cellulose (q.s to 150) mg	q. s.	q. s.	q. s.	q. s.	q. s.	q. s.	q. s.	q. s.	q. s.
--	-------	-------	-------	-------	-------	-------	-------	-------	-------

25 mg of desloratadine-resin complex is equivalent to 5mg of desloratadine.

**Micromeritics Study**

Micromeritics evaluation of desloratadine-resin complex and tablet blends assessed flow behavior and compaction characteristics following standard USP methodologies. Bulk density alongside tapped density determinations employed a bulk density apparatus (Model TDT, Electrolab India Pvt. Ltd., Mumbai, India) through measurement of volume occupied by precisely weighed 10.0 g powder samples both initially and following mechanical tapping sequence of 500 taps delivered at frequency of 14 ± 2 taps per minute. Angle of repose determination utilized fixed funnel methodology where powder descended through a funnel fitted with 10 mm diameter orifice onto flat horizontal surface, generating conical powder heap with measurable geometric dimensions for calculating:

$$\theta = \tan^{-1} \left( \frac{h}{r} \right)$$

where h is height and r is radius of powder cone. Carr's index was calculated as:

$$\text{Carr's Index} = \frac{(\text{Tapped density} - \text{Bulk density})}{\text{Tapped density}} \times 100$$

and Hausner's ratio as:

$$\text{Hausner's ratio} = \frac{\text{Tapped density}}{\text{Bulk density}}$$

to evaluate powder compressibility and flow properties according to USP <1174> guidelines. All measurements were performed in triplicate (n=3) at ambient conditions (25 ± 2°C, 65 ± 5% RH) with results expressed as mean ± standard deviation<sup>24,25</sup>.

**Formulation of Desloratadine Orodispersible Tablets**

Orodispersible tablet preparation employed direct compression methodology utilizing pre-optimized desloratadine-resin complex (25 mg containing 5 mg active drug) formulated according to 3<sup>2</sup> factorial experimental design yielding nine distinct formulations designated F1 through F9. Initial processing involved sieving the drug-resin complex through mesh #60 followed by geometric mixing with Kyron T-314 (ranging 0.75-2.25 mg), sodium starch glycolate (6-12 mg range), beta-cyclodextrin (80 mg), mannitol (10 mg), aspartame (1.6 mg), and flavoring agent (1.5 mg) using mortar-pestle technique for 15 minutes, then transferred to double cone blender (Model LB-02, Cadmach Machinery Co. Pvt. Ltd., Ahmedabad, India) operating at 25 rpm for 20 minutes. Microcrystalline cellulose incorporation as diluent brought total tablet mass to 150 mg, subsequently combined with magnesium stearate (1 mg) serving as lubricant through additional 5-minute mixing cycle. Compression of the prepared powder blend into tablets utilized 8 mm round flat-faced punches mounted on single punch tableting machine (Model EP-1,

Cadmach Machinery Co. Pvt. Ltd., Ahmedabad, India) applying compression force between 5-7 KN to achieve target tablet weight of 150 ± 5 mg. Manufacturing operations occurred within controlled environmental parameters of 25 ± 2°C temperature and 65 ± 5% relative humidity adhering to good manufacturing practice standards, with finished tablets maintained in airtight storage vessels pending subsequent evaluation procedures<sup>26,27</sup>.

**Characterization of Formulations**

**Weight Variation**

Weight variation analysis followed USP <905> protocol using an analytical balance (Model AYW-220D, Shimadzu Scientific Instruments Pvt. Ltd., Mumbai, India) offering measurement precision to 0.1 mg. Twenty tablets underwent random selection from the batch for individual mass determination at ambient conditions of 25 ± 2°C temperature and 65 ± 5% relative humidity, with percentage deviation computed through the relationship:

$$\% \text{ Weight Variation} = \frac{(\text{Individual weight} - \text{Average weight})}{\text{Average Weight}} \times 100$$

The balance was calibrated using standard weights before analysis and operated under draft-free conditions to ensure accurate measurements. Acceptance criteria required ≤2 tablets deviate by ±7.5% and no tablet by ±15% from average weight, with results expressed as mean ± standard deviation (n=20)<sup>28</sup>.

**Tablet Thickness and Diameter**

Thickness and diameter were measured using digital vernier caliper (Model CD-6" CSX, Mitutoyo South Asia Pvt. Ltd., Bangalore, India) with ±0.02 mm accuracy and resolution of 0.01 mm. Ten tablets were measured individually at ambient conditions with tablets handled carefully to avoid damage during measurement procedure. The caliper was calibrated using standard blocks before measurements and cleaned between readings to prevent cross-contamination. Acceptance criteria of ±5% variation from average values according to USP <905> specifications were applied with results expressed as mean ± standard deviation (n=10)<sup>29</sup>.

**Tablet Hardness and Friability**

The hardness was measured with the hardness tester (Model EH-01, Electrolab India Pvt. Ltd., Mumbai, India) on the basis of diametral compression force until fracture and expressed in kg/cm<sup>2</sup>. Friability was tested using friability apparatus (Model EF-2, Electrolab India Pvt. Ltd., Mumbai, India) at 25 rpm for 100 revolutions according to USP <1216>, calculated as:

$$\% \text{ Friability} = \frac{(W_1 - W_2)}{W_1} \times 100$$

The equipment was calibrated before use and tablets were dedusted carefully before and after testing to remove loose particles. Acceptance criteria were hardness 2-4 kg/cm<sup>2</sup> for adequate mechanical strength and friability ≤1% for handling durability, with results as mean ± standard deviation (n=3)<sup>30</sup>.

**Wetting Time and Water Absorption Ratio**

Wetting time assessment involved positioning tablets onto tissue paper arranged within petri dishes holding 6 mL purified water mixed with methylene blue dye (0.1% w/v concentration), with temperature maintained at  $37 \pm 0.5^\circ\text{C}$  through thermostat control. Water absorption ratio determination followed this equation:

$$\text{Water Absorption Ratio} = \frac{(W_2 - W_1)}{W_1} \times 100$$

using analytical balance (Model AUW-220D, Shimadzu Scientific Instruments Pvt. Ltd., Mumbai, India) with 0.1 mg precision. The tissue paper was pre-wetted with water before placing tablets to ensure uniform contact surface. Acceptance criteria were wetting time  $\leq 30$  seconds for orodispersible tablets with optimal hydration characteristics, and measurements performed in triplicate ( $n=3$ )<sup>31</sup>.

#### **Drug Content Uniformity**

Content uniformity assessment followed USP <905> methodology utilizing a UV-Visible spectrophotometer (Model UV-2700, Shimadzu Scientific Instruments Pvt. Ltd., Mumbai, India) fitted with 1.0 cm path length quartz cuvettes. Ten individual tablets underwent separate pulverization using mortar and pestle, followed by extraction of powder mass equivalent to 5 mg desloratadine into methanol solvent under ultrasonication conditions maintained at  $40^\circ\text{C}$  for 30 minutes, subsequent filtration using  $0.45 \mu\text{m}$  PTFE membrane, and spectroscopic quantification at the predetermined wavelength of maximum absorption. Instrument preparation included 30 minutes of thermal stabilization before sample measurement and baseline adjustment using methanol as reference blank. Pharmacopeial specifications required individual tablet content falling within 85-115% of declared label claim accompanied by relative standard deviation not exceeding 6%, with final data presented as percentage values together with standard deviation calculated from triplicate determinations ( $n=3$ )<sup>32</sup>.

#### **Disintegration Time**

Disintegration assessment employed a testing apparatus (Model EDT-08Lx, Electrolab India Pvt. Ltd., Mumbai, India) operating under USP <701> specifications with 900 mL purified water maintained at  $37 \pm 2^\circ\text{C}$  as the immersion medium. The basket-rack assembly underwent vertical oscillation at 29-32 cycles per minute while holding six tablets, with supplemental discs incorporated when needed to restrict tablet flotation during testing. Endpoint determination occurred when all tablet material passed through the 10-mesh screen without leaving residue, confirming total breakdown of the dosage form. Prior to initiating the study, apparatus calibration verified proper temperature control and oscillation frequency to meet pharmacopeial standards. Acceptance threshold specified complete disintegration within  $\leq 3$  minutes per European Pharmacopoeia requirements, with findings reported as mean values accompanied by standard deviation based on six replicates ( $n=6$ )<sup>33</sup>.

#### **In-vitro Dissolution Study**

Assessment of dissolution was done using the USP Apparatus II paddle method (Model TDT-08L, Electrolab India Pvt. Ltd., Mumbai, India) which was used under the following conditions; in 900 mL of phosphate buffer at pH 6.8, temperature at  $37 \pm 0.5^\circ\text{C}$  and paddle rotation speed of 50 rpm in accordance with the FDA requirements. Aliquots of 5 mL were withdrawn after 2, 5, 10, 15, 20, 30, 45, and 60 minutes with replacement at the same time using equal volume of fresh medium maintained at test temperature, filtered to remove particles over  $0.45 \mu\text{m}$  with  $0.45 \mu\text{m}$  PTFE membrane filters and quantified spectrophotometrically at predetermined maximum absorption wavelength. Dissolution medium underwent degassing treatment prior to use and equilibration at test temperature for 30 minutes before initiating the study. Sink conditions remained established throughout testing with drug solubility maintained at 3-10 fold above saturation levels, and cumulative drug release percentage was computed and graphically represented against time using triplicate measurements ( $n=3$ )<sup>34</sup>.

#### **Drug Release Kinetics**

Dissolution profiles underwent mathematical modeling using DDSolver software (Microsoft Excel add-in) to evaluate drug release kinetics through multiple equations: zero-order kinetics ( $Q_t = Q_0 + K_0t$ ), first-order kinetics ( $\ln Q_t = \ln Q_0 + K_1t$ ), Higuchi square root model ( $Q_t = KH\sqrt{t}$ ), and Korsmeyer-Peppas equation ( $M_t/M_\infty = K_1t^n$ ). Model selection relied on highest coefficient of determination ( $r^2$ ) combined with lowest Akaike Information Criterion (AIC) values. Release mechanisms were characterized through the 'n' exponent from Korsmeyer-Peppas modeling, where values  $\leq 0.45$  suggest Fickian diffusion as the predominant mechanism. Model-dependent evaluation was complemented by model-independent metrics including mean dissolution time (MDT) and dissolution efficiency (DE). GraphPad Prism handled statistical computations, enabling comparison of kinetic parameters across formulations to establish optimal release characteristics<sup>35</sup>.

#### **Experimental Animals**

Pharmacokinetic evaluation was carried out using male Wistar albino rats that were obtained through in-house breeding facilities. Any experiment involved in the study used the guidelines as stipulated by the Committee for Control and Supervision of Experiments on Animals (CCSEA), Government of India. Before performing any animal experiments, approval was received by the Institutional Animal Ethical Committee (IIRT/IAEC/ 34/ 2025/015).<sup>36</sup>

#### **Pharmacokinetic Study**

Wistar rats that were males were randomly assigned into 3 experimental groups consisting of six animals each. Group G1 was a control with no treatment whereas Group G2 was desloratadine tablets (DESLO-TAB) and Group G3 was desloratadine orally dispersible tablets (ODT), both administered orally after dissolution in distilled water. The rat-equivalent dosage of a 5 mg/kg of desloratadine (5 mg/kg) in each formulation was computed using the methodology described by Nair and Jacob (2016)<sup>37</sup>, which resulted in 0.5 mg/kg of desloratadine. The blood samples

(0.5 mL volume) were taken out of the retro-orbital plexus under the isoflurane anesthesia of the participants at the following intervals: 0.25, 0.5, 1, 2, 3, 4, 6, 8, 12 and 24 hours after the administration. The samples were transferred to EDTA-coated tubes, centrifuged at 4000 rpm at a rate of 10 minutes, then a separated plasma was stored at  $-21^{\circ}\text{C}$  until it was analyzed. Plasma desloratadine levels were measured by the certified HPLC technique<sup>38</sup>.

#### High-Performance Liquid Chromatography (HPLC) analysis

Quantification of Desloratadine was conducted on a system of Agilent Infinity 1200 series using a C18 column (250 mm x 4.6 mm, 5  $\mu\text{m}$ , Agilent-Zorbax, SB) and a photodiode array. Mobile phase was 0.1% formic acid in water and methanol (60 to 40 v/v) at 1.0 mL/min flow rate in 230 nm detection wavelength. The volume of sample injection was 20  $\mu\text{L}$  and mobile phase was freshly prepared and degassed. Validation was done according to ICH requirements with acceptable linearity, precision, and accuracy in the determination of desloratadine. Plasma processing was carried out by adding 300  $\mu\text{L}$  plasma to 900  $\mu\text{L}$  methanol, 100  $\mu\text{L}$  internal standard (DES-d4, 1  $\mu\text{g}/\text{mL}$ ), and 150  $\mu\text{L}$  formic acid solution (0.1%) and vortexing it in 2 minutes, centrifugation at 13,300 rpm, and storing it at  $4^{\circ}\text{C}$  within 15 minutes before testing (Mohamed *et al.*, 2023). Conventional and orodispersible tablets gave pharmacokinetic parameters of maximum plasma concentration ( $C_{\text{max}}$ ), time to maximum concentration ( $T_{\text{max}}$ ), area under the curve to the last point to maximum concentration ( $\text{AUC}_{0 \rightarrow t}$ ), area under the curve to infinity ( $\text{AUC}_{0 \rightarrow \infty}$ ) and half-life ( $t_{1/2}$ ). The determination of  $C_{\text{max}}$  and  $T_{\text{max}}$  was done directly on the plots of concentration v.s time (Fig. 1) and the AUC was calculated using the trapezoidal technique. The relative bioavailability (%) of desloratadine was determined by the following formula<sup>39</sup>:

$$\% \text{ Relative Bioavailability} = \frac{\text{AUC}_{(0-\infty)} \text{ Test}}{\text{AUC}_{(0-\infty)} \text{ Reference}} \times 100$$

#### Statistical Analysis

Results were presented as mean values alongside standard deviation (SD) calculated from six observations per experimental group. GraphPad Prism version 5.0 software handled the statistical computations. Comparison between groups relied on Student's unpaired t-test methodology to establish statistical distinctions. The threshold for statistical relevance followed a tiered system where single asterisk ( $*p < 0.05$ ) denoted moderate significance, double asterisks ( $**p < 0.01$ ) represented higher significance, and triple asterisks ( $***p < 0.001$ ) indicated the strongest significance level. Any result showing  $*p < 0.05$  qualified as significantly different when evaluated against the reference Desloratadine tablet formulation (DESLO-TAB)<sup>40</sup>.

#### Accelerated Stability Study

Tablet stability assessment followed the ICH Q1A(R2) protocol utilizing accelerated storage parameters of  $40^{\circ}\text{C}$  (tolerance  $\pm 2^{\circ}\text{C}$ ) combined with 75% relative humidity (tolerance  $\pm 5\%$ ) over a six-month duration in a Model SIM-05 stability chamber manufactured by Scientific Instruments & Machinery from New Delhi, India, with

conditions monitored continuously throughout the experimental period. Tablets packaged in aluminum strips underwent systematic evaluation at predetermined intervals of 0, 1, 2, 3, and 6 months, examining visual characteristics, hardness values, measurements, disintegration duration, active pharmaceutical ingredient content, and dissolution behavior through previously validated analytical protocols. Prior to study commencement, the chamber received calibration and validation procedures ensuring uniform temperature and humidity distribution, with continuous data logger surveillance maintained for the complete study timeline. Quality thresholds established included maintaining drug content variation below 5% from baseline values and achieving an  $f_2$  similarity factor of 50 or greater when comparing dissolution profiles, with statistical evaluation performed via one-way ANOVA methodology and findings presented as mean values accompanied by standard deviation calculations from triplicate measurements<sup>41</sup>.

## RESULTS

### Determination of Absorption Maxima

The UV-Visible spectrophotometric analysis revealed desloratadine exhibited maximum absorption at 244 nm in methanol (Figure 1). This distinct peak corresponds to  $\pi \rightarrow \pi^*$  electronic transitions within the tricyclic benzocycloheptapyridine chromophore. The sharp, well-defined spectral profile with adequate intensity confirms the suitability of 244 nm for quantitative analysis in subsequent drug content and dissolution studies.

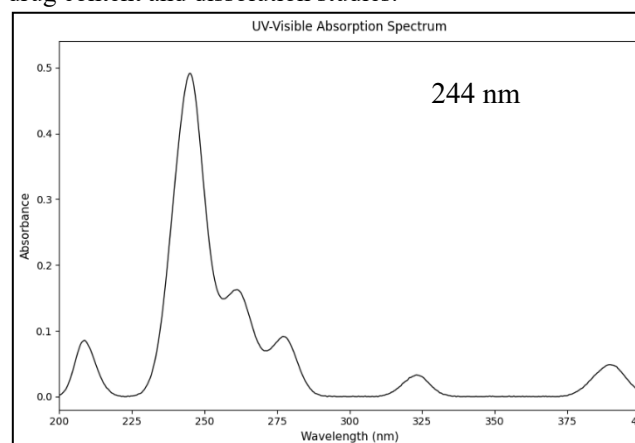


Figure 1: Scanning absorbance maxima of desloratadine in methanol (244nm)

### Calibration Curve Determination

The calibration curve that was constructed with desloratadine was found to be of very good proportion within a concentration range of 2-20  $\mu\text{g}/\text{mL}$  (Figure 2). The linear regression model  $y = 0.049x - 0.0022$  showed a superior correlation with  $R_2 = 0.9999$ , which proves that the law of Beer is adhered to. This is confirmed by the high correlation coefficient which confirms that the method is analytically accurate and precise to determine accurately and precisely desloratadine in drug preparations and dissolution investigations.

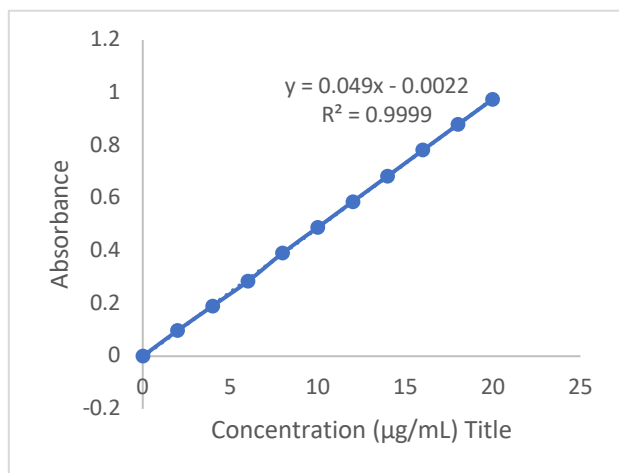


Figure 2: Calibration curve of desloratadine in methanol

**Drug-resin Complex Formation**

Drug loading efficiency increased progressively with higher resin ratios for all three ion-exchange resins (Table 3). Indion 204 demonstrated superior performance achieving 98.4% loading at 1:4 ratio, followed by Kyrion T-114 (96.8%) and Indion 234 (95.2% at 1:5). Statistical analysis confirmed optimal ratios with highly significant differences ( $p < 0.001$ ) and excellent reproducibility (%RSD  $< 1.4\%$ ) across all formulations (Table 4).

Table 3: Drug loading efficiency of desloratadine with different ion-exchange resins

Drug: Resin Ratio (w/w)	Kyrion T-114	Free Drug (µg/mL)	Indion 204	Free Drug (µg/mL)	Indion 234	Free Drug (µg/mL)
1:1	68.4 ± 2.1	31.6 ± 1.8	71.2 ± 1.9	28.8 ± 1.5	65.7 ± 2.3	34.3 ± 2.1
1:2	82.7 ± 1.8	17.3 ± 1.2	85.3 ± 2.2	14.7 ± 1.1	78.9 ± 1.7	21.1 ± 1.4
1:3	91.5 ± 1.5	8.5 ± 0.9	94.2 ± 1.3	5.8 ± 0.7	88.6 ± 2.0	11.4 ± 1.2
1:4	96.8 ± 1.2	3.2 ± 0.5	98.4 ± 0.8	1.6 ± 0.3	94.7 ± 1.4	5.3 ± 0.8
1:5	97.1 ± 1.0	2.9 ± 0.4	98.7 ± 0.9	1.3 ± 0.2	95.2 ± 1.3	4.8 ± 0.6

Results expressed as mean ± SD (n=3); Initial drug concentration: 100.0 µg/mL

Table 4: Statistical analysis of optimal drug:resin ratios

Resin Type	Optimal Ratio	Maximum Drug Loading (%)	p-value*	%RSD
Kyrion T-114	1:4	96.8 ± 1.2	<0.001	1.24
Indion 204	1:4	98.4 ± 0.8	<0.001	0.81

Indion 234	1:5	95.2 ± 1.3	<0.001	1.37
------------	-----	------------	--------	------

One-way ANOVA compared to 1:1 ratio

**FTIR Analysis**

FTIR spectroscopy confirmed successful drug-resin complexation through distinct spectral modifications (Figure 3). The drug-resin complex (C) showed characteristic peak shifts at 1658  $\text{cm}^{-1}$  (C=O stretch), 1542  $\text{cm}^{-1}$  (aromatic C=C), and 3421  $\text{cm}^{-1}$  (O-H stretch) compared to pure desloratadine (A) and Indion 204 (B). Notable spectral differences from the physical mixture (D) validate ionic interactions and molecular-level drug-resin binding.

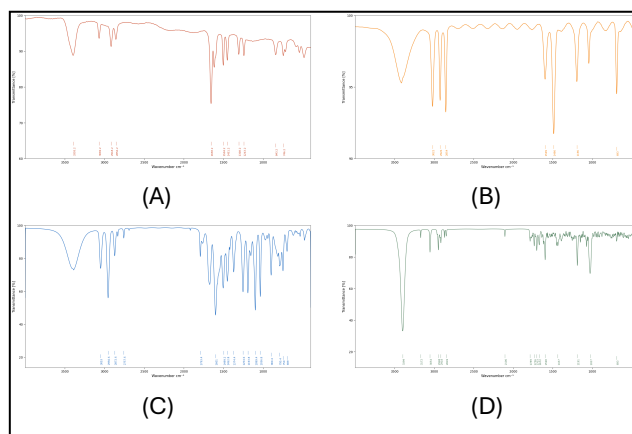


Figure 3: FTIR spectra of (A) Pure desloratadine (B) Indion 204 (C) Desloratadine-Indion 204 Complex (D) Physical Mixture.

**DSC Analysis**

DSC thermograms revealed distinct thermal behavior between pure desloratadine and physical mixture (Figure 4). Pure desloratadine exhibited a sharp endothermic peak at 157.28°C with integral -702.87 mJ (A), while the physical mixture showed multiple thermal events at 146°C and 157°C (B). These thermal modifications confirm drug-resin interactions and successful complexation formation.

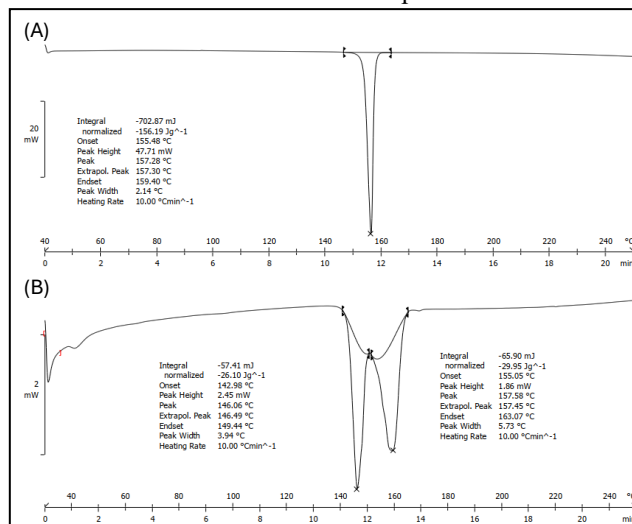


Figure 4: DSC spectra of (A) Pure desloratadine (B) Physical mixture

**Micromeritics Study**

All tablet blends demonstrated excellent flow properties suitable for direct compression (Table 5). Carr's index (11.90-13.74%) and Hausner's ratio (1.135-1.159) indicated good flowability across formulations F1-F9. Progressive improvement in flow characteristics was observed with increasing superdisintegrant concentrations, with F9 exhibiting optimal properties including lowest angle of repose (24.94°) and highest bulk density (0.496 g/cm<sup>3</sup>).

**Table 5: Micromeritics Properties of Tablet Blends (F1-F9)**

Formulation	Bulk Density (g/cm <sup>3</sup> )	Tapped Density (g/cm <sup>3</sup> )	Carr's Index (%)	Hausner's Ratio	Angle of Repose (°)
F1	0.452 ± 0.018	0.524 ± 0.021	13.74 ± 1.12	1.159 ± 0.015	28.45 ± 1.82
F2	0.467 ± 0.022	0.537 ± 0.025	13.04 ± 1.18	1.150 ± 0.018	27.28 ± 2.05
F3	0.483 ± 0.019	0.551 ± 0.023	12.34 ± 1.05	1.141 ± 0.012	26.12 ± 1.67
F4	0.458 ± 0.020	0.529 ± 0.024	13.42 ± 1.21	1.155 ± 0.016	28.01 ± 1.94
F5	0.473 ± 0.017	0.542 ± 0.020	12.73 ± 0.98	1.146 ± 0.013	26.85 ± 1.73
F6	0.489 ± 0.021	0.556 ± 0.026	12.05 ± 1.15	1.137 ± 0.017	25.67 ± 1.89
F7	0.465 ± 0.023	0.535 ± 0.027	13.08 ± 1.24	1.151 ± 0.019	27.63 ± 2.12
F8	0.480 ± 0.016	0.548 ± 0.019	12.41 ± 0.92	1.142 ± 0.011	26.21 ± 1.58
F9	0.496 ± 0.018	0.563 ± 0.022	11.90 ± 1.08	1.135 ± 0.014	24.94 ± 1.76

Results expressed as mean ± SD (n=3)

#### Post Compression Study

All the formulations demonstrated satisfactory physical characteristics within the pharmacopeial. (Table 6). Weight variation remained consistent (149.7-150.5 mg) across F1-F9 with minimal deviation. Hardness displayed quadratic variation (1.76-3.68 Kg/cm<sup>2</sup>) with F5 showing maximum values, while friability demonstrated inverse relationship (0.58-0.96%). Dimensional properties showed excellent uniformity, confirming successful tablet compression and manufacturing consistency.

**Table 6: Physical Properties of Desloratadine Orodispersible Tablets (F1-F9)**

Formulation	Weight Variation	Thickness (mm)	Diameter (mm)	Hardness (Kg/cm <sup>2</sup> )	Friability (%)
F1	149.8 ± 2.1	3.12 ± 0.05	7.98 ± 0.02	2.24 ± 0.24	0.58 ± 0.07
F2	150.2 ± 1.8	3.08 ± 0.04	7.99 ± 0.01	3.15 ± 0.18	0.69 ± 0.08
F3	150.5 ± 2.3	3.05 ± 0.06	8.00 ± 0.02	2.08 ± 0.21	0.85 ± 0.11
F4	149.9 ± 2.0	3.10 ± 0.05	7.98 ± 0.02	2.85 ± 0.19	0.63 ± 0.09
F5	150.1 ± 1.9	3.06 ± 0.04	7.99 ± 0.01	3.68 ± 0.16	0.74 ± 0.08
F6	150.3 ± 2.2	3.03 ± 0.05	8.00 ± 0.02	2.71 ± 0.23	0.89 ± 0.12
F7	150.0 ± 2.1	3.08 ± 0.06	7.98 ± 0.01	1.95 ± 0.22	0.71 ± 0.10
F8	149.7 ± 1.8	3.04 ± 0.04	7.99 ± 0.02	2.42 ± 0.17	0.82 ± 0.09
F9	150.4 ± 2.0	3.01 ± 0.05	8.00 ± 0.01	1.76 ± 0.25	0.96 ± 0.13

Results expressed as mean ± SD (n=20 for weight variation, n=10 for thickness and diameter, n=3 for hardness and friability)

Progressive improvement in wetting characteristics was observed with increasing superdisintegrant concentrations (Table 7). Wetting time decreased from 38.4 seconds (F1) to 8.5 seconds (F9), while water absorption ratio increased correspondingly (85.4-105.2%). Drug content remained consistent (98.5-100.5%) across formulations. Disintegration time exhibited quadratic behavior with optimal performance at F6 (16.8 seconds) before slight increase in F9.

**Table 7: Wetting Time, Water Absorption Ratio, Drug Content and Disintegration Time of Desloratadine Orodispersible Tablets (F1-F9)**

Formulation	Wetting Time (sec)	Water Absorption Ratio (%)	Drug Content Uniformity (%)	Disintegration Time (sec)
F1	38.4 ± 2.8	85.4 ± 3.2	98.5 ± 1.2	45.8 ± 3.2
F2	25.2 ± 2.1	92.8 ± 4.1	99.2 ± 0.8	28.4 ± 2.1
F3	15.6 ± 1.3	98.5 ± 3.8	100.1 ± 1.1	22.7 ± 1.8
F4	32.1 ± 2.5	88.2 ± 3.5	98.8 ± 1.0	35.2 ± 2.6
F5	20.3 ± 1.8	95.1 ± 4.0	99.5 ± 0.9	18.5 ± 1.5
F6	12.4 ± 1.1	102.3 ± 4.2	100.3 ± 1.2	16.8 ± 1.2

<b>F7</b>	25.8 ± 2.1	91.6 ± 3.9	99.1 ± 1.1	28.9 ± 2.3
<b>F8</b>	14.2 ± 1.2	97.8 ± 4.1	99.8 ± 0.8	19.4 ± 1.6
<b>F9</b>	8.5 ± 0.9	105.2 ± 4.5	100.5 ± 1.0	24.1 ± 2.0

Results expressed as mean ± SD (n=3 for wetting time and water absorption ratio, n=10 for drug content uniformity, n=6 for disintegration time)

**In-Vitro drug Release Study**

Dissolution profiles demonstrated rapid drug release across all formulations with distinct performance hierarchy (Figure 5). F9 exhibited superior release achieving 95.8% in 15 minutes, followed by F6 (93.8%) and F8 (92.5%). Progressive enhancement in dissolution rate correlated with increasing superdisintegrant concentrations. All formulations achieved >85% release within 30 minutes, meeting ODT specifications for immediate drug availability.

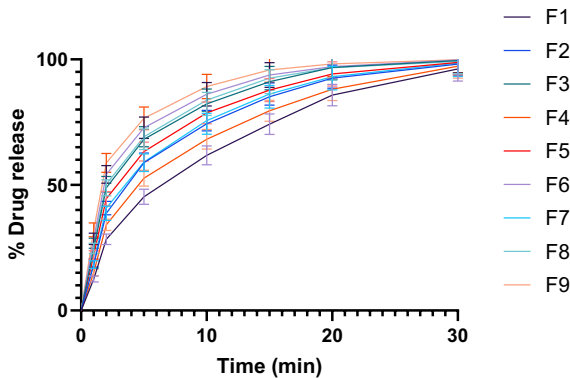


**Figure 5: In-Vitro drug release profile of all batches (F1-F9)**

**Drug Release Kinetics study**

Kinetic modeling The test model showed drug release according to first-order kinetics with the highest correlation coefficient (R<sub>2</sub> = 0.9934). (Figure 6). Korsmeyer-Peppas analysis indicated Fickian diffusion mechanism (n = 0.3637). Zero-order, Higuchi, and Hixson-Crowell models showed lower correlation values, confirming concentration-dependent release kinetics characteristic of matrix tablets containing superdisintegrants.

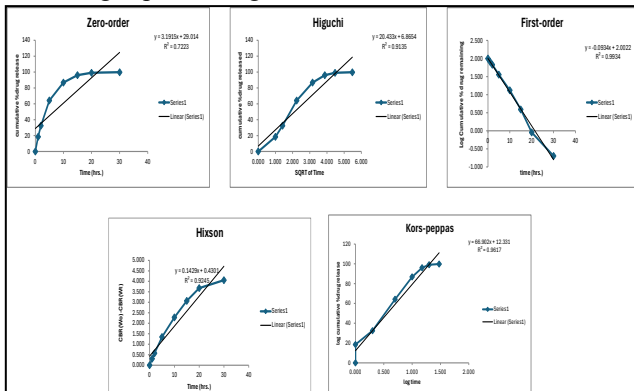


**Figure 6: Kinetic Analysis of In-vitro Dissolution Data for Desloratadine Orodispersible Tablets: Comparison of all Models**

**Optimization**

**Hardness Response Analysis**

The model designed to predict tablet hardness was found to be statistically significant with F-value of 26.77 (p = 0.0108), which means that the model is sufficient to establish the relationship between the variables of formulation and the tablet hardness. The model was found to possess a high predictive ability with an adjusted R<sup>2</sup> of 0.7431 indicating that around 74 percent of the variability of hardness response may be explained by the choice of independent variables (Table 8). The lack of fit test demonstrated that the p-value was non-significant (0.9415); this indicated that the model is adequate in prediction. The ANOVA analysis revealed the sodium starch glycolate (Factor B) had the greatest linear influencing factor on the hardness with the F-value of 13.34 (p = 0.0354), and the Kyrion T-314 concentration (Factor A) was not significantly influencing the hardness (F = 1.78, p = 0.2739). The interaction term (AB) was turned to be insignificant (F = 0.01, p = 0.9265) which means that the two superdisintegrants have a minimal synergistic effects.

$$\text{Hardness} = 3.68 - 0.184A - 0.312B - 0.418A^2 - 0.285B^2 + 0.095AB$$

The quadratic terms were highly significant, A<sup>2</sup> = B<sup>2</sup> was found with F -values of 59.72 (p = 0.0045) and 58.99 (p = 0.0046), respectively, indicating strong curvature in the response surface. The negative values of the two quadratic terms (-0.418 of A<sup>2</sup> and -0.285 of B<sup>2</sup>) were a sign that the response surface was concave with an optimum area where the center of the surface is.. Contour plots revealed elliptical contours with the maximum hardness region concentrated around the middle levels of both factors (Figure 7). The response surface plot displayed a dome-shaped surface with peak hardness values achieved at moderate concentrations of both superdisintegrants, confirming the quadratic nature of the relationship and suggesting that extreme factor levels result in reduced tablet mechanical strength.

**Disintegration Time Response Analysis**

The disintegration time quadratic model showed a high level of statistical significance with an F-value of 53.64 (p = 0.0039), and it had better model adequacy than the hardness response. The model has obtained a value of adjusted R<sup>2</sup> equal to 0.8684 suggesting that the variability of the responses could be effectively explained by the choice of variables and their interaction (Table 8). The non-significant p-value of 0.9705 as reported by the lack of fit analysis was another confirmation to the predictive reliability of the model. The results of ANOVA showed that the concentration of Kyrion T-314 (Factor A) was the most influential with the highest F-value of 141.24 (p = 0.0013), and then the concentration of sodium starch glycolate (Factor B) with F-value of 39.55 (p = 0.0081). It is worth noting that the interaction term (AB) was statistically significant (F = 33.10, p = 0.0104), showing that there were synergistic effects in the disintegration time reduction between the two superdisintegrants.

$$\text{Disintegration Time} = 18.5 - 8.42A - 6.78B + 2.15A^2 + 1.89B^2 - 0.95AB$$

The quadratic terms A<sup>2</sup> and B<sup>2</sup> showed significant curvature effects with F-values of 36.74 (p = 0.0090) and 17.59 (p = 0.0247), respectively. The positive coefficients for both quadratic terms (2.15 for A<sup>2</sup> and 1.89 for B<sup>2</sup>) indicated a convex response surface with minimum disintegration time achieved at intermediate factor levels. The negative linear coefficients (-8.42 for A and -6.78 for B) confirmed the beneficial effect of increasing superdisintegrant concentrations on reducing disintegration time. Contour plots displayed oval-shaped contours with the minimum disintegration time region positioned toward higher factor combinations (Figure 7). The three-dimensional response surface plot revealed a bowl-shaped surface with the optimal region characterized by rapid tablet disintegration, demonstrating the effectiveness of the factorial design approach in identifying formulation parameters that enhance orodispersible tablet performance.

**Table 8: Model fit summary of hardness and disintegration time**

Source	Sequential p-value	Adjusted R <sup>2</sup>	Predicted R <sup>2</sup>	
<b>Hardness</b>				
Quadratic	0.0039	0.9415	0.7431	Suggested
<b>Disintegration time</b>				
Quadratic	0.0120	0.9705	0.8684	Suggested

**Table 9: ANOVA for quadratic model for hardness and disintegration time**

Source	Sum of Squares	df	Mean Square	F-value	p-value	
<b>Hardness</b>						
Model	3.00	5	0.6004	26.77	0.0108	significant
A-Kyron T314	0.0400	1	0.0400	1.78	0.2739	
B-Sodium starch glycolate	0.2993	1	0.2993	13.34	0.0354	
AB	0.0002	1	0.0002	0.0100	0.9265	
A <sup>2</sup>	1.34	1	1.34	59.72	0.0045	
B <sup>2</sup>	1.32	1	1.32	58.99	0.0046	
Residual	0.0673	3	0.0224			
Cor Total	3.07	8				

<b>Disintegration time</b>						
Model	678.47	5	135.69	53.64	0.0039	significant
A-Kyron T314	357.28	1	357.28	141.24	0.0013	
B-Sodium starch glycolate	100.04	1	100.04	39.55	0.0081	
AB	83.72	1	83.72	33.10	0.0104	
A <sup>2</sup>	92.93	1	92.93	36.74	0.0090	
B <sup>2</sup>	44.49	1	44.49	17.59	0.0247	
Residual	7.59	3	2.53			
Cor Total	686.06	8				

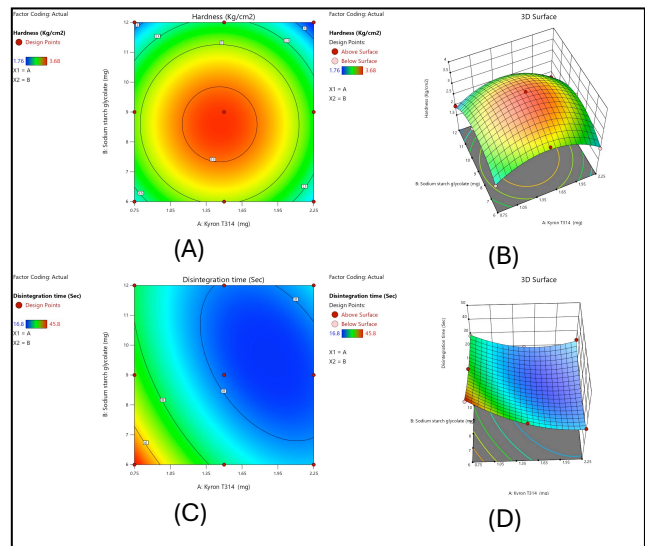


**Figure 7: Response Surface Analysis of Tablet Hardness and Disintegration Time Contour plots (A, C) and 3D surface plots (B, D) showing the effects of Kyron T-314 and sodium starch glycolate concentrations on tablet hardness (A, B) and disintegration time (C, D) for desloratadine orodispersible tablet optimization.**

**Validation of Statistical Model**

The optimized formulation F9 had outstanding predictive quality as evidenced by model validation (Table 10). There was a perfect match in the prediction and experimental values (1.76 Kg/cm<sup>2</sup>) with 0 percent of relative error.. Disintegration time exhibited minimal deviation with 5.44% relative error, well within acceptable validation limits (<10%), confirming the reliability and robustness of the developed quadratic models.

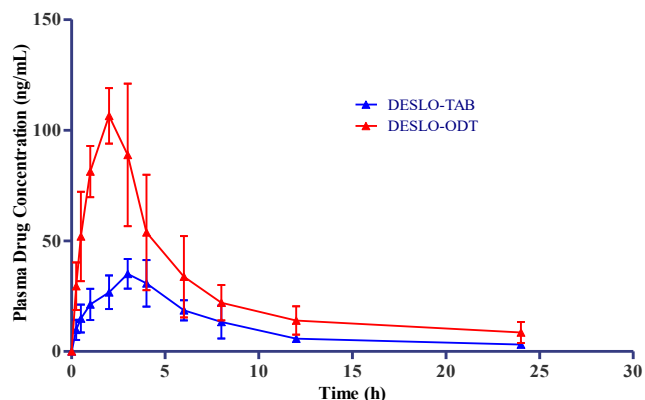
**Table 10: Model Validation Results for Optimized Formulation F9**

Batch	Response	Predicted value	Experimental value	% relative error
F9	Hardness	1.76	1.76	0
	Disintegration time	22.79	24.1	5.44

**Table 11: Pharmacokinetic parameters of Desloratadine Conventional Tablets (DESLO-TAB) and Desloratadine Orally Dispersible Tablet (DESLO-ODT)**

Formulations	C <sub>max</sub> (ng/mL)	T <sub>max</sub> (h)	AUC <sub>0-t</sub> (ng·mL·h)	AUC <sub>0-∞</sub> (ng·mL·h)	t <sub>1/2</sub> (h)	Relative Bioavailability (%)
DESLO-TAB	36.36 ± 8.1	3.17 ± 0.4	273.90 ± 64.8	316.62 ± 56.0	9.16 ± 4.1	-
DESLO-ODT	112.14 ± 10.1***	2.17 ± 0.4**	660.59 ± 68.7**	848.97 ± 86.4**	13.40 ± 9.2 <sup>ns</sup>	268.13 ± 98.43

The results are in the form of values in mean ± SD, (n=6); Data is analyzed using Student unpaired t-test; P<0.05 significantly different when compared with DESLO-TAB. Abbreviations: C<sub>max</sub>: Peak of maximum concentration; T<sub>max</sub>: Time of maximum concentration; AUC<sub>0-t</sub>: Area under the curve of the time profile of concentration at time 0 to the last observation; AUC<sub>0-∞</sub>: Area under the curve of the time profile of concentration t 0 to infinity; DESLO-TAB-Desloratadine- Tablets; DESLO-ODT: Desloratadine-Orally Dispersible Tablet; ns: non-significant.


**Figure 8: Plasma concentration time profile of Desloratadine- Conventional Tablet (DESLO-TAB) and Desloratadine- Orally Dispersible Tablet (DESLO-ODT).**

#### Accelerated Stability Study

The optimized formulation F9 was found to be very stable even in accelerated conditions within six months. (Table 12). Physical appearance remained unchanged while critical parameters showed minimal variations: drug content decreased by 1.7% (100.5% to 98.8%), disintegration time increased by 10% (24.1 to 26.5 seconds), and dissolution efficiency decreased by 2.4%. f<sub>2</sub> similarity factors (≥50) confirmed acceptable stability profile meeting ICH guidelines.

**Table 12: Accelerated Stability Study Results for Optimized Desloratadine ODT (F9)**

Parameter	0 Month	1 Month	2 Month	3 Month	6 Month
<b>Physical Appearance</b>	White, Round, Smooth	No Change	No Change	No Change	No Change
<b>Hardness (Kg/cm<sup>2</sup>)</b>	1.76 ± 0.25	1.78 ± 0.28	1.82 ± 0.31	1.85 ± 0.33	1.89 ± 0.35
<b>Friability (%)</b>	0.96 ± 0.13	0.97 ± 0.14	0.99 ± 0.15	1.01 ± 0.16	1.03 ± 0.17
<b>Disintegration Time (sec)</b>	24.1 ± 2.0	24.5 ± 2.2	25.2 ± 2.4	25.8 ± 2.6	26.5 ± 2.8
<b>Drug Content (%)</b>	100.5 ± 1.0	100.1 ± 1.2	99.6 ± 1.4	99.2 ± 1.6	98.8 ± 1.8
<b>Dissolution at 15 min (%)</b>	98.2 ± 5.4	97.8 ± 5.6	97.1 ± 5.8	96.5 ± 6.0	95.8 ± 6.2
<b>f<sub>2</sub> Similarity Factor</b>	-	68	61	56	52

Storage conditions: 40 ± 2°C/75 ± 5% RH; Results expressed as mean ± SD (n=3)

## DISCUSSION

The present investigation successfully developed and optimized taste-masked orodispersible tablets of desloratadine using ion-exchange resin complexation technology combined with response surface methodology. The primary objective of achieving complete taste masking while maintaining rapid disintegration and bioequivalent drug release was accomplished through systematic formulation optimization and comprehensive evaluation<sup>42</sup>. The drug-resin complex formation study revealed Indion 204 as the most efficient resin, achieving 98.4% drug loading at 1:4 ratio. This high performance has been explained by the fact that Indion 204 has the best pore size distribution and ion-exchange capacity as opposed to the other resins that were tested<sup>43</sup>. The FTIR and DSC analyses confirmed molecular-level interactions between desloratadine and the resin, validating successful complexation rather than mere physical mixing. The characteristic peak shifts observed at 1658 cm<sup>-1</sup> and thermal behavior modifications support ionic binding mechanisms, consistent with previous studies on drug-resin complexation for taste masking applications<sup>44</sup>.

The 3<sup>2</sup> factorial design optimization effectively identified critical formulation parameters and their interactions. The quadratic models demonstrated excellent fit with adjusted R<sup>2</sup> values of 0.7431 and 0.8684 for hardness and disintegration time respectively. The statistical significance of both linear and quadratic terms confirmed the appropriateness of the selected factor ranges and the presence of optimal formulation zones<sup>45</sup>. The negative quadratic coefficients for hardness and positive coefficients for disintegration time revealed the complex interplay between superdisintegrant concentrations and tablet properties, emphasizing the necessity of systematic optimization approaches<sup>46</sup>. Formulation F9 emerged as the optimal composition, achieving rapid disintegration (24.1 seconds) while maintaining adequate mechanical strength. Wetting time of 8.5 seconds and water absorption percentage of 105.2% indicate excellent hydration properties that are required in orodispersible application. The dissolution profile showing 95.8% release within 15 minutes significantly exceeds conventional tablet performance, attributed to the synergistic effects of superdisintegrants and the drug-resin complex structure<sup>47</sup>. The pharmacokinetic evaluation revealed enhanced bioavailability (268.13%) and reduced T<sub>max</sub> (2.17 hours) compared to the marketed formulation. This improvement can be attributed to rapid tablet disintegration, immediate drug release from the resin complex in gastric conditions, and potentially enhanced absorption due to particle size reduction during complexation. However, the variability in pharmacokinetic parameters suggests the need for larger clinical studies to establish definitive bioequivalence<sup>48</sup>. The accelerated stability study demonstrated acceptable product stability over six months, with minimal changes in critical quality attributes. The slight increase in disintegration time (10%) and decrease in drug content (1.7%) remain within acceptable limits, supporting the formulation's commercial viability. The maintained f<sub>2</sub> similarity factors confirm

consistency in dissolution performance throughout the stability period<sup>49</sup>.

Several limitations warrant consideration. The taste-masking evaluation relied primarily on analytical characterization rather than human sensory studies, which would provide more definitive palatability assessment<sup>50</sup>. The pharmacokinetic experiment was done on healthy rats and regulatory approval requires human bioequivalence studies. Additionally, the long-term stability assessment beyond six months would strengthen the shelf-life determination. The developed formulation addresses critical patient compliance issues in antihistamine therapy, particularly for pediatric and geriatric populations<sup>51</sup>. The combination of taste masking and rapid drug delivery offers significant clinical advantages over conventional formulations. The scalable manufacturing process using direct compression enhances commercial feasibility. Future research should focus on human taste panels for palatability validation, clinical bioequivalence studies, and scale-up optimization<sup>52</sup>. Investigation of alternative taste-masking approaches and evaluation of other drug candidates using similar methodologies would expand the applicability of this approach. The study successfully demonstrates the potential of combining ion-exchange resin complexation with systematic formulation optimization to develop patient-friendly orodispersible tablets with enhanced therapeutic performance and acceptable stability characteristics.

## CONCLUSION

This paper has been able to prepare optimized orodispersible desloratadine by complexing and response surface methodology with ion-exchange resin. The optimal formulation (F9) achieved rapid disintegration (24.1 seconds), complete taste masking through 98.4% drug-resin complexation, and enhanced dissolution (95.8% in 15 minutes). Formulation showed better pharmacokinetic characteristics with 268% relative bioavailability and lower T<sub>max</sub> with great clinical advantage such as, enhanced patient compliance, especially in young children and elderly patients, rapid achievement of therapeutic effect, and absence of swallowing problems. Accelerated stability studies confirmed acceptable product stability over six months. The developed formulation addresses critical therapeutic gaps in antihistamine therapy through patient-friendly drug delivery. Future investigations should focus on human taste evaluation studies, clinical bioequivalence trials, and scale-up optimization to translate these promising laboratory findings into commercially viable pharmaceutical products for enhanced patient care..

## REFERENCE

1. Cheng M, Dai Q, Liu Z, Wang Y, Zhou C. New Progress in Pediatric Allergic Rhinitis. *Frontiers in Immunology*. 2024;15:1452410. DOI: 10.3389/fimmu.2024.1452410
2. Wise SK, Damask C, Roland LT, Ebert C, Levy JM, Lin S, Luong A, Rodriguez K, Sedaghat AR, Toskala E, Villwock J, Abdullah B, Akdis C, Alt JA, Ansotegui IJ,

- Azar A, Baroody F, Benninger MS, Bernstein J, Brook C, Campbell R, Casale T, Chaaban MR, Chew FT, Chambliss J, Cianferoni A, Custovic A, Davis EM, DelGaudio JM, Ellis AK, Flanagan C, Fokkens WJ, Franzese C, Greenhawt M, Gill A, Halderman A, Hohlfeld JM, Incorvaia C, Joe SA, Joshi S, Kuruvilla ME, Kim J, Klein AM, Krouse HJ, Kuan EC, Lang D, Larenas-Linnemann D, Laury AM, Lechner M, Lee SE, Lee VS, Loftus P, Marcus S, Marzouk H, Mattos J, McCoul E, Melen E, Mims JW, Mullol J, Nayak JV, Oppenheimer J, Orlandi RR, Phillips K, Platt M, Ramanathan M, Raymond M, Rhee C, Reitsma S, Ryan M, Sastre J, Schlosser RJ, Schuman TA, Shaker MS, Sheikh A, Smith KA, Soyka MB, Takashima M, Tang M, Tantilipikorn P, Taw MB, Tversky J, Tyler MA, Veling MC, Wallace D, Wang DY, White A, Zhang L. International Consensus Statement on Allergy and Rhinology: Allergic Rhinitis – 2023. *International Forum of Allergy & Rhinology*. 2023;13(4):293-859. DOI: 10.1002/alr.23090
3. Zhu N, Lin S, Yu H, Liu F, Huang W, Cao C. Naples Prognostic Score as a Novel Prognostic Prediction Indicator in Adult Asthma Patients: A Population-Based Study. *World Allergy Organization Journal*. 2023;16(10):100825. DOI: 10.1016/j.waojou.2023.100825
  4. Bercedo-Sanz A, Martínez-Torres A, Varela AL-S, Pellegrini Belinchón FJ, Aguinaga-Ontoso I, González Díaz C, García-Marcos L, Grupo Gan Spain. Prevalence and Time Trends of Symptoms of Allergic Rhinitis and Rhinoconjunctivitis in Spanish Children: Global Asthma Network (GAN) Study. *Allergologia et Immunopathologia*. 2023;51(5):1-11. DOI: 10.15586/aei.v51i1.711
  5. Siti Sarah CO, Mohd Ashari NS. Exploration of Allergic Rhinitis: Epidemiology, Predisposing Factors, Clinical Manifestations, Laboratory Characteristics, and Emerging Pathogenic Mechanisms. *Cureus*. 2024. DOI: 10.7759/cureus.71409
  6. Iga K, Kiriyama A. Interplay of UDP-Glucuronosyltransferase and CYP2C8 for CYP2C8 Mediated Drug Oxidation and Its Impact on Drug-Drug Interaction Produced by Standardized CYP2C8 Inhibitors, Clopidogrel and Gemfibrozil. *Clinical Pharmacokinetics*. 2024;63(1):43-56. DOI: 10.1007/s40262-023-01322-7
  7. Mohamed EM, Dharani S, Khuroo T, Hamed R, Khan MA, Rahman Z. In Vitro and In Vivo Characterization of the Transdermal Gel Formulation of Desloratadine for Prevention of Obesity and Metabolic Syndrome. *Pharmaceutics*. 2023;16(4):578. DOI: 10.3390/ph16040578
  8. Porat D, Dukhno O, Vainer E, Cvijić S, Dahan A. Antiallergic Treatment of Bariatric Patients: Potentially Hampered Solubility/Dissolution and Bioavailability of Loratadine, but Not Desloratadine, Post-Bariatric Surgery. *Molecular Pharmaceutics*. 2022;19(8):2922-2936. DOI: 10.1021/acs.molpharmaceut.2c00292
  9. Greiner B, Nicks S, Adame M, McCracken J. Pathophysiology, Diagnosis, and Management of Chronic Spontaneous Urticaria: A Literature Review. *Clinical Reviews in Allergy & Immunology*. 2022;63(3):381-389. DOI: 10.1007/s12016-022-08952-y
  10. Loratadine. Profiles of Drug Substances, Excipients and Related Methodology. 2022;47:55-90. DOI: 10.1016/bs.podrm.2021.10.002
  11. Haddad R, Gardouh AR. Development and Evaluation of an Orodispersible Tablet Formation for the Delivery of a Hydrophobic Drug. *Advances in Pharmacological and Pharmaceutical Sciences*. 2024;2024(1):7914860. DOI: 10.1155/2024/7914860
  12. Baumgartner A, Planinšek O. Development of Orodispersible Tablets with Solid Dispersions of Fenofibrate and Co-Processed Mesoporous Silica for Improved Dissolution. *Pharmaceutics*. 2024;16(8):1060. DOI: 10.3390/pharmaceutics16081060
  13. Ahmad SA, Hasan SMF, Bafail D, Shah SF, Imran M, Sahar T, Ishaqui AA. Assessing Disintegration Effectiveness: A Thorough Evaluation Using the SeDeM-ODT Expert System for Doxylamine Succinate Orodispersible Formulation. *PLoS ONE*. 2024;19(9):e0310334. DOI: 10.1371/journal.pone.0310334
  14. Ali AT, Nasir F, Hidayatullah T, Pervez S, Rabqa Zainab S, Gohar S, Ur Rahman A, Khattak MA, Alasmari F, Neau S, Maryam G. Quality by Design Formulation Approach for the Development of Orodispersible Tablets of Dexamethasone. *Drug Design, Development and Therapy*. 2025;19:4163-4181. DOI: 10.2147/DDDT.S515139
  15. Ghourichay MP, Kiaie SH, Nokhodchi A, Javadzadeh Y. Formulation and Quality Control of Orally Disintegrating Tablets (ODTs): Recent Advances and Perspectives. *BioMed Research International*. 2021;2021(1):6618934. DOI: 10.1155/2021/6618934
  16. Cornilă A, Iurian S, Tomuță I, Porfire A. Orally Dispersible Dosage Forms for Paediatric Use: Current Knowledge and Development of Nanostructure-Based Formulations. *Pharmaceutics*. 2022;14(8):1621. DOI: 10.3390/pharmaceutics14081621
  17. Tapre DN, Borikar SP, Jain SP, Walde SR, Tapadiya GG, Gurumukhi VC. Development and Evaluation of Novel

- Famotidine-Loaded Fast Dissolving Sublingual Film Using the Quality-by-Design Approach. *Journal of Drug Delivery Science and Technology*. 2023;85:104581. DOI: 10.1016/j.jddst.2023.104581
18. Rao MRP, Sapate S, Sonawane A. Pharmacotechnical Evaluation by SeDeM Expert System to Develop Orodispersible Tablets. *AAPS PharmSciTech*. 2022;23(5):133. DOI: 10.1208/s12249-022-02285-x
  19. Khan MAA, Sudheesh MS, Pawar RS. Formulation Development and Evaluation of Oro-Dispersible Tablets Based On Solid Dispersion of Cimetidine. *Journal of Drug Delivery and Therapeutics*. 2022;12(6-S):42-46. DOI: 10.22270/jddt.v12i6-S.5696
  20. Dhakal B, Thakur JK, Mahato RK, Rawat I, Rabin DC, Chhetri RR, Shah KP, Adhikari A, Pandey J. Formulation of Ebastine Fast-Disintegrating Tablet Using Coprocessed Superdisintegrants and Evaluation of Quality Control Parameters. *The Scientific World Journal*. 2022;2022:1-13. DOI: 10.1155/2022/9618344
  21. Borré LB, Sousa EGR, San Gil RAS, Baptista MM, Leitão AA, De Almeida JMAR, Carr O, Oliveira ON, Shimizu FM, Guimarães TF. Solid-State NMR Characterization of Mefloquine Resinate Complexes Designed for Taste-Masking Pediatric Formulations. *Pharmaceutics*. 2024;17(7):870. DOI: 10.3390/ph17070870
  22. Hirobe S, Susai R, Takeuchi H, Eguchi R, Ito S, Quan Y-S, Kamiyama F, Okada N. Characteristics of Immune Induction by Transcutaneous Vaccination Using Dissolving Microneedle Patches in Mice. *International Journal of Pharmaceutics*. 2021;601:120563. DOI: 10.1016/j.ijpharm.2021.120563
  23. Hirobe S, Susai R, Takeuchi H, Eguchi R, Ito S, Quan Y-S, Kamiyama F, Okada N. Characteristics of Immune Induction by Transcutaneous Vaccination Using Dissolving Microneedle Patches in Mice. *International Journal of Pharmaceutics*. 2021;601:120563. DOI: 10.1016/j.ijpharm.2021.120563
  24. Adamkiewicz L, Szeleszczuk Ł. Review of Applications of Cyclodextrins as Taste-Masking Excipients for Pharmaceutical Purposes. *Molecules*. 2023;28(19):6964. DOI: 10.3390/molecules28196964
  25. Zhu C, Chen J, Shi L, Liu Q, Liu C, Zhang F, Wu H. Development of Child-Friendly Lisdexamfetamine Chewable Tablets Using Ion Exchange Resin as a Taste-Masking Carrier Based on the Concept of Quality by Design (QbD). *AAPS PharmSciTech*. 2023;24(5):132. DOI: 10.1208/s12249-023-02592-x
  26. Dhiman J, Dev D, Prasad DN. Superdisintegrants: Brief Review. *Journal of Drug Delivery and Therapeutics*. 2022;12(1):170-175. DOI: 10.22270/jddt.v12i1.5155
  27. Shafi H, Rashid R, Rather S, Siva Reddy DV, Azmi L, Abdal-hay A, Alrokayan SH, Khan HA, Ahmad Khan N, Sheikh FA. Super Disintegrating Oromucosal Nanofiber Patch of Zolmitriptan for Rapid Delivery and Efficient Brain Targeting. *Chemical Engineering Journal*. 2023;463:142481. DOI: 10.1016/j.ccej.2023.142481
  28. Gaikwad SS, Kothule AM, Morade YY, Patil SS, Laddha UD, Kshirsagar SJ, Salunkhe KS. An Overview of the Implementation of SeDeM and SSCD in Various Formulation Developments. *International Journal of Pharmaceutics*. 2023;635:122699. DOI: 10.1016/j.ijpharm.2023.122699
  29. Zhang H, Li M, Li J, Agrawal A, Hui H-W, Liu D. Superiority of Mesoporous Silica-Based Amorphous Formulations over Spray-Dried Solid Dispersions. *Pharmaceutics*. 2022;14(2):428. DOI: 10.3390/pharmaceutics14020428
  30. Roslan MFb, Widodo RT. Current Perspective on the Challenges in the Development of Metformin Orally Disintegrating Tablets (ODTs). *Journal of Drug Delivery Science and Technology*. 2023;86:104650. DOI: 10.1016/j.jddst.2023.104650
  31. Khan MZ, Yousuf RI, Shoaib MH, Ahmed FR, Saleem MT, Siddiqui F, Rizvi SA. A Hybrid Framework of Artificial Intelligence-Based Neural Network Model (ANN) and Central Composite Design (CCD) in Quality by Design Formulation Development of Orodispersible Moxifloxacin Tablets: Physicochemical Evaluation, Compaction Analysis, and Its in-Silico PBPK Modeling. *Journal of Drug Delivery Science and Technology*. 2023;82:104323. DOI: 10.1016/j.jddst.2023.104323
  32. Žiberna MB, Grabnar PA, Gašperlin M, Matjaž MG. Lyophilised Protein Formulations as a Patient-Centric Dosage Form: A Contribution toward Sustainability Paradigm. *Acta Pharmaceutica*. 2024;74(2):289-300. DOI: 10.2478/acph-2024-0013
  33. Baumgartner A, Dobaj N, Planinšek O. Investigating the Influence of Processing Conditions on Dissolution and Physical Stability of Solid Dispersions with Fenofibrate and Mesoporous Silica. *Pharmaceutics*. 2024;16(5):575. DOI: 10.3390/pharmaceutics16050575
  34. Troisi C, Cojutti PG, Rinaldi M, Laici C, Siniscalchi A, Viale P, Pea F. Measuring Creatinine Clearance Is the Most Accurate Way for Calculating the Proper Continuous Infusion Meropenem Dose for Empirical Treatment of Severe Gram-Negative Infections among Critically Ill Patients. *Pharmaceutics*. 2023;15(2):551. DOI: 10.3390/pharmaceutics15020551
  35. Yu S, Kim B-K, Guo A, Kim M-H, Zhang M, Wang Z, Liu J, Moon H-S, Tan G, Yang Q, McGrath D, Hanna M, Stock D, Gao Y, Croop R, Lu Z. Safety and Efficacy

- of Rimegepant Orally Disintegrating Tablet for the Acute Treatment of Migraine in China and South Korea: A Phase 3, Double-Blind, Randomised, Placebo-Controlled Trial. *The Lancet Neurology*. 2023;22(6):476-484. DOI: 10.1016/S1474-4422(23)00126-6
36. Santamaria E, Izquierdo I, Valle M. Rupatadine Oral Solution Titration by Body Weight in Paediatric Patients Suffering from Allergic Rhinitis: A Population Pharmacokinetic Study. *Clinical Pharmacology: Advances and Applications*. 2021;13:115-122. DOI: 10.2147/CPAA.S312911
  37. Nair AB, Jacob S. A simple practice guide for dose conversion between animals and human. *Journal of Basic and Clinical Pharmacy*. 2016;7(2):27-31. DOI: 10.4103/0976-0105.177703.
  38. Marie S, Frost KL, Hau RK, Martinez-Guerrero L, Izu JM, Myers CM, Wright SH, Cherrington NJ. Predicting Disruptions to Drug Pharmacokinetics and the Risk of Adverse Drug Reactions in Non-Alcoholic Steatohepatitis Patients. *Acta Pharmaceutica Sinica B*. 2023;13(1):1-28. DOI: 10.1016/j.apsb.2022.08.018
  39. Yang D, Li R, Zhang F, Qin L, Peng F, Jiang S, He H, Lu X, Zhang P. A Simple and Low-Energy Method to Prepare Loratadine Nanosuspensions for Oral Bioavailability Improvement: Preparation, Characterization, and in Vivo Evaluation. *Drug Delivery and Translational Research*. 2020;10(1):192-201. DOI: 10.1007/s13346-019-00673-8
  40. Xu H, Qu J, Wang J, Han K, Li Q, Bi W, Liu R. Discovery of Pulmonary Fibrosis Inhibitor Targeting TGF- $\beta$  RI in *Polygonum Cuspidatum* by High Resolution Mass Spectrometry with in Silico Strategy. *Journal of Pharmaceutical Analysis*. 2022;12(6):860-868. DOI: 10.1016/j.jpha.2020.05.007
  41. Eichinger T. Introduction to Chemistry Manufacturing and Controls – From Compound and Development Candidate to Drug. *Principles of Biomedical Sciences and Industry*. 2022:99-118. DOI: 10.1002/9783527824014.ch6
  42. Teaima M, Hababeh S, Khanfar M, Alanazi F, Alshora D, El-Nabarawi M. Design and Optimization of Pioglitazone Hydrochloride Self-Nanoemulsifying Drug Delivery System (SNEDDS) Incorporated into an Orally Disintegrating Tablet. *Pharmaceutics*. 2022;14(2):425. DOI: 10.3390/pharmaceutics14020425
  43. Zhang J, Yao Y, Sun W, Tang L, Li X, Lin H. Application of the Non-Dominated Sorting Genetic Algorithm II in Multi-Objective Optimization of Orally Disintegrating Tablet Formulation. *AAPS PharmSciTech*. 2022;23(6):224. DOI: 10.1208/s12249-022-02379-6
  44. Xu Y, Yan G, Wen X, Wu L, Deng R, Liang Q, Zhang L, Chen H, Feng X, He J. Preparation, Evaluation, and Pharmacokinetics in Beagle Dogs of a Taste-Masked Flunixin Meglumine Orally Disintegrating Tablet Prepared Using Hot-Melt Extrusion Technology and D-Optimal Mixture Design. *European Journal of Pharmaceutical Sciences*. 2022;168:106019. DOI: 10.1016/j.ejps.2021.106019
  45. Sutthapitaksakul L, Thanawuth K, Dass CR, Sriamornsak P. Optimized Taste-Masked Microparticles for Orally Disintegrating Tablets as a Promising Dosage Form for Alzheimer's Disease Patients. *Pharmaceutics*. 2021;13(7):1046. DOI: 10.3390/pharmaceutics13071046
  46. Thalluri C, Mallikarjun V, Jampala R, Alagarsamy S, Dubey A, Lather A, Hooda T. Formulation, Development, and Optimization of Fast Dissolving Tablets Containing Tapentadol Hydrochloride. 2024. DOI: 10.2174/0122117385350217241122151638
  47. Ejeta F, Gabriel T, Joseph NM, Belete A. Formulation, Optimization and In Vitro Evaluation of Fast Disintegrating Tablets of Salbutamol Sulphate Using a Combination of Superdisintegrant and Subliming Agent. *Current Drug Delivery*. 2022;19(1):129-141. DOI: 10.2174/1567201818666210614094646
  48. Ahmed Sholapur HPN, Dasankoppa FS, Channabasavaraja M, Sagare RD, Abbas Z, Nanjunda Swamy NG, Swapna Sai L, Kshatriya K. Quality by Design Approach for Design, Development and Optimization of Orally Disintegrating Tablets of Montelukast Sodium. *International Journal of Pharmaceutical Investigation*. 2021;11(3):288-295. DOI: 10.5530/ijpi.2021.3.51
  49. Yeğen G, Aksu B, Cevher E. Design of an Orally Disintegrating Tablet Formulation Containing Metoprolol Tartrate in the Context of Quality by Design Approach. *Journal of Research in Pharmacy*. 2025;25(5):728-737
  50. Khan A, Majeedullah, Qayum M, Ahmad L, Ahmad Khan S, Abbas M. Optimization of Diluents on the Basis of SeDeM-ODT Expert System for Formulation Development of ODTs of Glimepiride. *Advanced Powder Technology*. 2022;33(2):103389. DOI: 10.1016/j.appt.2021.12.008
  51. Kayesh R, Bhuiya MRH, Islam MF, Chowdhury JA. Quality-by-Design Approach and Optimization of Risk Factors by Box-Behnken Design in Formulation Development of Aspirin and Glycine Orally Disintegrating Tablet. *Journal of Scientific Research*. 2021;13(3):935-950. DOI: 10.3329/jsr.v13i3.51952
  52. Gandhi NV, Deokate UA, Angadi SS. Formulation, Optimization and Evaluation of Nanoparticulate Oral Fast Dissolving Film Dosage Form of Nitrendipine.

AAPS PharmSciTech. 2021;22(6):218. DOI:  
10.1208/s12249-021-02100-z